Title	Fundamental Studies on Electron Beam Welding of Heat resistant Superalloys for Nuclear Plants (Report IV) : Effect of High Temperature He on the Properties of Weld Joints(Materials, Metallurgy, Weldability)
Author(s)	Arata, Yoshiaki; Terai, Kiyohide; Nagai, Hiroyoshi et al.
Citation	Transactions of JWRI. 1979, 8(1), p. 33-41
Version Type	VoR
URL	https://doi.org/10.18910/3815
rights	
Note	

Fundamental Studies on Electron Beam Welding of Heat resistant Superalloys for Nuclear Plants (Report IV) †
— Effect of High Temperature He on the Properties of Weld Joints —

Yoshiaki ARATA[*], Kiyohide TERAI[**], Hiroyoshi NAGAI[**], Shigeki SHIMIZU[**], Toshiichi AOTA[**]

and Takashi MURAKAMI[**]

Abstract

In this paper, corrosion behavior and change of structure of base metal, its electron beam and TIG weld zone of superalloys for nuclear plants in the environment of high temperature helium were made clear and compared with each other. As results, it has been clarified that the corrosion resistance of Hastelloy X is superior to the other superalloys and the corrosion resistance of electron beam weld zone is superior to TIG weld zone and nearly comparable to base metal.

KEY WORDS: (Electron Beam Welding) (Heat-resistant Superalloy) (Nuclear Plants) (Weld Joint)

1. Introduction

Such superalloys as Hastelloy type, Inconel type and Incoloy type for nuclear plants are used in helium environment at high temperature of about 1,000°C. It is expected that the quality of meterial will be deteriorated in use at high temperature in helium for many hours due to the corrosion and carbonization reaction on the surface of material which occur by means of minor impurity elements in helium, that is, H_2, H_2O, CO, CO_2, CH_4, and O_2. Moreover, it is expected that the structure and properties of material with change as a result of precipitation and cohesion process of carbides by aging. It is considered that such material changes caused in high temperature helium will have some effects on the material

strength in a long time. However, there are very few systematic reports on the material properties in high temperature helium, especially, there is no report on the properties of weld zone.

This paper discusses the quality changes of base metals of the above heat-resistant superalloys and their electron beam and TIG weld joints, resulting from the surface corrosion and precipitation process of carbides in high temperature helium.

2. Materials used and welding procedures

Table 1 shows the chemical composition and mechanical properties of such superalloys as Hastelloy type,

Table 1 Chemical composition and mechanical properties of superalloys used

Material	Thickness (mm)	☀ Melting Process	Final Heat Treatment	Grain Size (ASTM)	Mechanical Properties				Chemical Composition (%)														
					0.2%PS (Kg/mm²)	T.S (Kg/mm²)	El. (%)	R.A (%)	C	Si	Mn	P	S	Ni	Cr	Co	Mo	W	Nb+Ta	Al	Ti	B	Fe
Hastelloy X		AE	1100°Cx9Mim A.C	5~7	50.35	86.2	35.6	—	0.087	0.47	0.87	0.018	0.003		21.61	1.53	9.00	0.40	—	—	—	0.003	18.83
Inconel 625		AE	1000°Cx30Min W.Q	7~9	63.8	100.4	36.4	—	0.05	0.33	0.33	0.0004	<0.0005	Bal.	22.26	0.10	9.11	—	3.29	0.23	0.14	—	2.78
Inconel 617	2	V	1150°C x 6Min W.Q	4~6	40.5	81.2	52.6	45.6	0.07	0.15	0.07	—	0.007		21.99	12.53	9.06	—	—	0.98	—	—	0.22
Incoloy 800		V	1100°C x10Min W.Q	25	21.6	58.5	52.4	73.6	0.05	0.31	0.80	0.0012	0.0005	31.31	21.50	—	—	—	—	0.57	0.59	—	Bal
Incoloy 807		A	1150°C x 6Min W.Q	7~8	35.0	80.0	30.1	—	0.006	0.33	0.83	0.0003	0.0009	40.13	20.65	8.40	—	4.88	0.96	0.48	0.30	—	Bal

☀ AE: Air Melting followed by Electroslag Remelting, V: Vacuum Induction Melting, A: Air Melting

Inconel type and Incoloy type used. **Table 2** shows the chemical composition of filler metal used for TIG welding. Electron beam and TIG welding were respectively carried out in such conditions as shown in **Table 3** and **Table 4**.

Table 2 Chemical composition of filler metal for TIG welding used

Material	Chemical Composition (%)															
	C	Si	Mn	P	S	Ni	Cr	Co	Mo	W	Nb+Ta	Al	Ti	B	Fe	Cu
HastelloyX	0.07	0.42	0.35	0.013	<0.005	Bal.	21.56	1.00	8.97	0.51	—	—	—	0.002	17.80	—
Inconel625	0.015	0.32	0.32	0.004	<0.005		21.53	Tr.	8.86	—	3.74	0.16	0.14	—	2.62	—
Inconel617	0.08	0.16	0.03	—	<0.007		22.27	12.45	9.13	—	—	0.89	—	—	0.50	—
Inconel82	0.01	0.17	2.92	—	0.007		19.77	—	—	—	2.59	—	0.35	—	0.38	0.03
Incoloy800	0.09	0.14	3.55	0.002	0.007	34.17	20.25	—	—	—	—	0.24	0.27	—	Bal.	—
Incoloy807	0.06	0.38	0.75	0.002	0.009	39.16	20.62	7.93	—	4.89	—	0.39	0.46	—		—

Notes; Melting Process: Vacuum Induction Melting

Table 3 Electron beam welding conditions
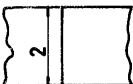
Joint Configuration	Welding Conditions					
	P_{ch} (Torr)	D_F (mm)	a_b	I_b (mA)	V_b (kv)	U_b' (cm/min)
	5×10^{-4}	225	1.04	20	100	160

Table 4 TIG welding conditions

Joint Configuration	Built-up Sequence	Welding Conditions						
		Pass	Size of Filler Metal (mm)	Welding Current (A)	Arc Voltage (V)	Welding Speed (mm/min)	Shield Gas Flow Rate (l/min)	
							Torch	Back-up
		1-2	1.2	60-70	9-10	50-60	6	10

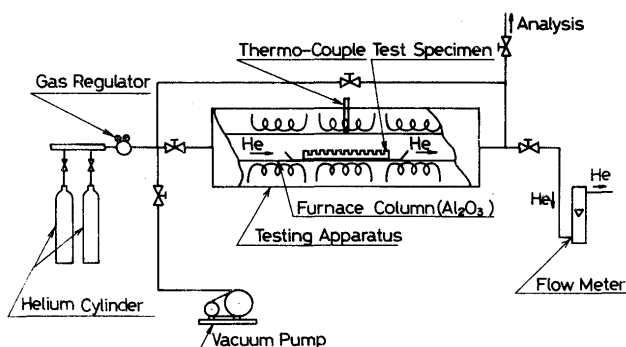Interpass Temperature: Max. 100°C

3. Experimental method

Fig. 1 Schematic diagram of horizontal type electric furnace

Figure 1 shows the schematic diagram of the corrosion test apparatus. The electric furnace is of horizontal type in which the furnace column is made of alumina. The inside diameter and uniform heating range of the furnace column are 105^ϕmm and $100^\phi \times 300^l$mm respectively.

The size of test specimen is $1^t \times 20 \times 10$mm. The weld joints were machined so as to position the weld bead at the center of test specimens and perpendicular to longitudinal direction. The test specimens were inserted one by one in a separate pot which is made of alumina and holed on the both sides to contact flowing helium to test specimens fluently. These pots were arranged in alumina jig which fitted the inside diameter of furnace column, and it was set up within a uniform heating range of the furnace column. The temperature of test specimens were checked continuously during the test and it was confirmed that the temperature of test specimens were all within an error range of $2°C$ of the specified test temperature.

The environment used for the test is HTR approximate helium[1]. Regarding the analysis of impurity elements in helium, a gas-chromatograph was used to analyze H_2, O_2, N_2, CH_4, CO and CO_2 and a hydrometer was used to analyze H_2O. The analysis was made both at the inlet and outlet of the electric furnace. **Table 5** shows the results of analysis. Internal pressure of the furnace was set at 1 kg/cm^2G. The flow rate of helium was set to 500 cc/min

Table 5 Impurity composition in helium

(PPM)

	H_2	CO	H_2O	CO_2	CH_4	O_2	N_2
Specification	200	100	2	1	<0.5	<1	<5
Analysis(Inlet)	207	100	2	<2	<5	<1	<5
Analysis(Outlet)	210 ~240	100 ~103	1~2	<5	Nil	<3	<6

$CO/CO_2, H_2/H_2O \fallingdotseq 100/1$ $(H_2)(CO_2)/(CO)(H_2O) \fallingdotseq 1$

for about 100 hours at an early stage of the test and later to 100 cc/min.

Before starting the test, the inside of furnace column was made below 1×10^{-5} Torr, substituted with HTR approximate helium and heated to the specified test temperature. After the aging test of 500 and 1000 hours at 800°C, 500, 1000 and 3000 hours at 900°C and 500 and 1000 hours at 1000°C, in helium, some investigations were carried out on the weight gain, the appearance of oxide film and composition and structure of surface parts of test specimens, and also structure and hardness of the matrix of test specimens comparing to the data of not aged test specimens.

4. Experimental results and discussions

4.1 Weight gain

The test environment is mild oxidizing environment as the oxidizing potential, $\log(P_{H_2}/P_{H_2O})$ is 2.0 to 2.4.
Figure 2 shows the boundaries of oxide formation of metals, and each curve indicates that the metal is not oxidized on the higher side of $\log(P_{H_2}/P_{H_2O})$ while the metal is oxidized on the lower side of $\log(P_{H_2}/P_{H_2O})$. Accordingly, in the case of this test environment, Al, Ti, Si, Mn and Cr are selectively oxidized in that order, and Ni and Fe which are main compositions, are not oxidized.

The weight gain of base metal of superalloys after aging test is shown in **Fig. 3** as an example. Each plot shows an average value of 2 or 3 test specimens. In either case, the results indicate a parabolic weight gain vs aging time.

There is no significant difference in weight gain among the electron beam weld joints, the TIG weld joints and the base metal for each material. When it is compared by material, Hastelloy X which is a solid solution strengthened superalloy, is the most excellent among the materials used, generally showing the smallest weight gain at the respective test temperatures. Inconel 625 which is also a solid solution strengthened superalloy, shows the smaller weight gain second to Hastelloy X at 800 and 900°C but the largest weight gain at 1000°C. On the other hand, Inconel 617, Incoloy 800 and Incoloy 807 which are
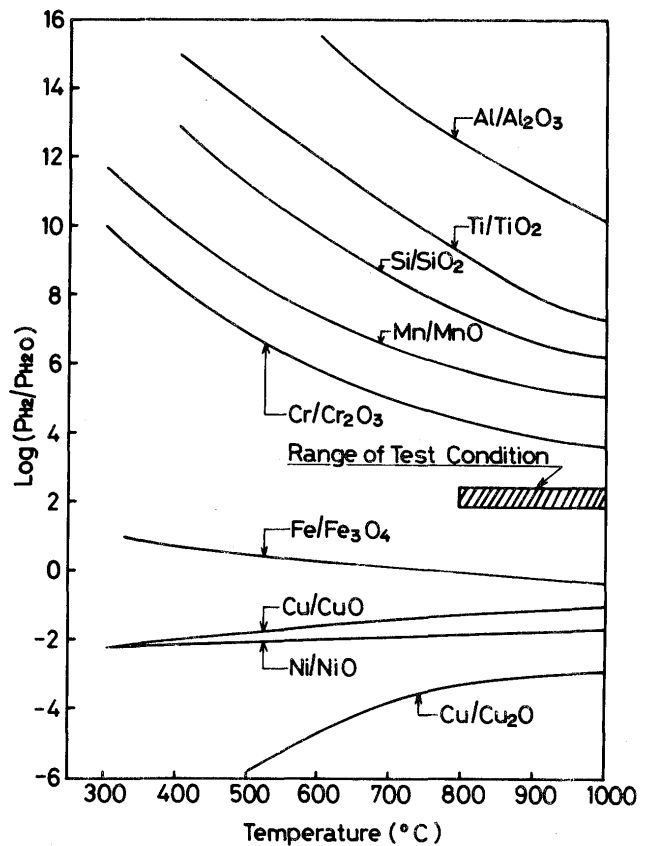

Fig. 2 Relation between temperature and oxidation potential for metals
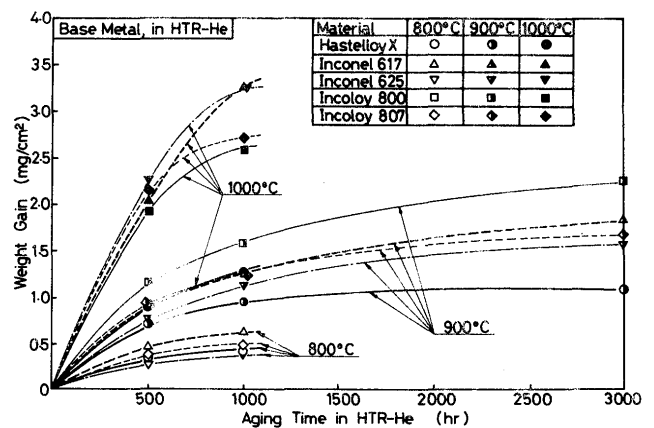

Fig. 3 Relation between aging time and weight gain for base metal

precipitation strengthened superalloys by adding Al and Ti, show larger weight gain at the respective test temperature than Hastelloy X.

Figure 4 shows the relation between the test tempera-
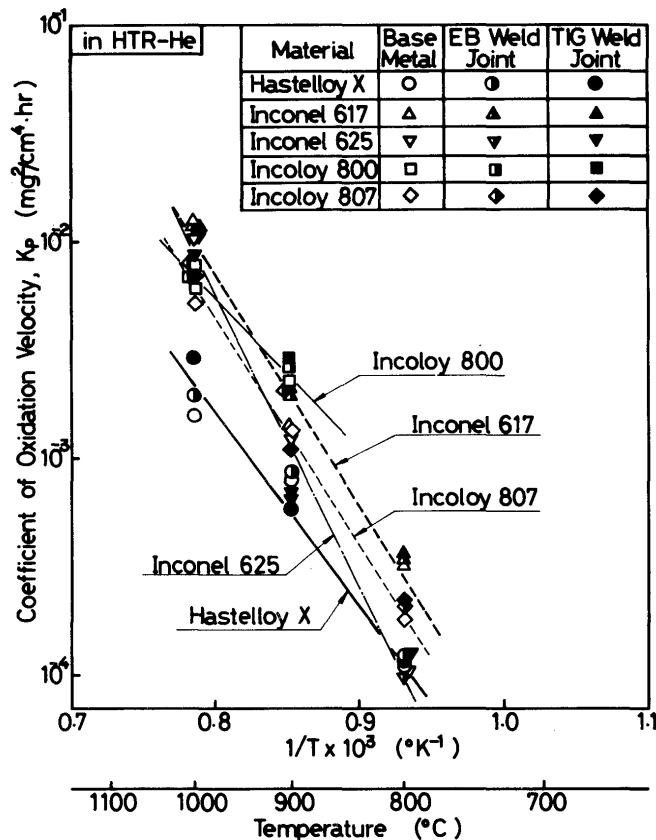

Fig. 4 Relation between temperature and coefficient of oxidation velocity

ture and the coefficient of oxidation velocity for each material used. Assuming that a weight gain follows the parabolic rule, the coefficient of oxidation velocity Kp was calculated from the following relation.

$$\Delta W^2 = K_p.t + C,$$

where

ΔW: Weight gain (mg/cm^2) at the aging time t,

t: Aging time (hr),

K_p, C: Constant

The temperature dependence of K_p on each material shows nearly linear relation in the Arrhenius' indication. When K_p values of base metal and its electron beam and TIG weld Joints for each material are compared, there is no significant difference regardless of some dispersions. K_p values of Hastelloy X at the respective test temperatures are smaller than the values of other materials, and a slope against temperature is gentle, showing that an

increasing rate of weight gain with a rise of temperature is smaller than those of other materials.

4.2 Internal oxidation

Since the precipitation strengthened superalloys as Inconel 617, Incoloy 800 and Incoloy 807 maintain the high temperature strength by precipitating Ni_3Al and Ni_3Ti in the matrix. Al and Ti are added as minor compositions to such superalloys. Al and Ti are selectively oxidized in the environment of high temperature helium containing oxidizing impurity elements and are locally precipitated as Al or Ti oxide at grain boundaries of materials to cause the internal oxidation. It is considered that the internal oxidation progresses with the lapse of time to detriorate the strength of materials and that it is one of important factors in case the material properties in high temperature helium containing minor impurity elements are to be evaluated.

Table 6 shows the microphotographs of cross-sections

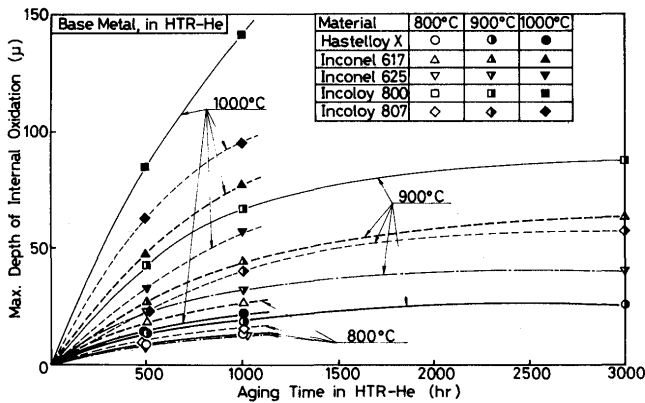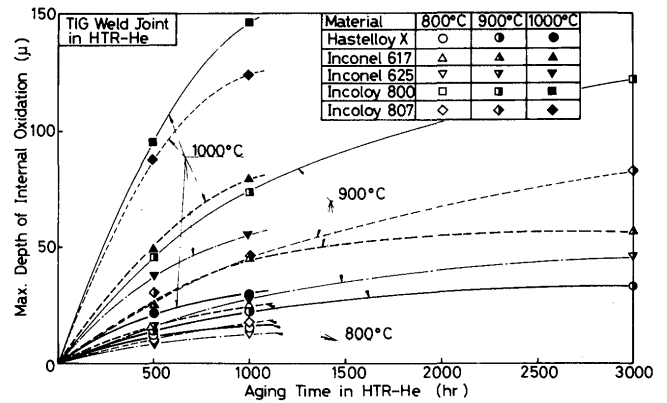Table 6 Internal oxidation for base and weld metals aged at 900°C in helium for 3000 hr

of test specimens which were aged at 900°C in helium for 3,000 hours as an example of the internal oxidation under this test. These photograghs indicate that the grain boundaries of the material are mainly corroded and degrees of internal oxidation of Hastelloy X and Inconel 625 are smaller than those of Inconel 617, Incoloy 800 and Incoloy 807. **Table 7** shows the results of EPMA analysis of Inconel 617 aged at 900°C in helium for 3,000

Table 7 Distribution of compositions in cross-section of Inconel 617 aged at 900°C in helium for 3000 hr by EPMA

Fig. 7 Relation between aging time and max. depth of internal oxidation for TIG weld metal
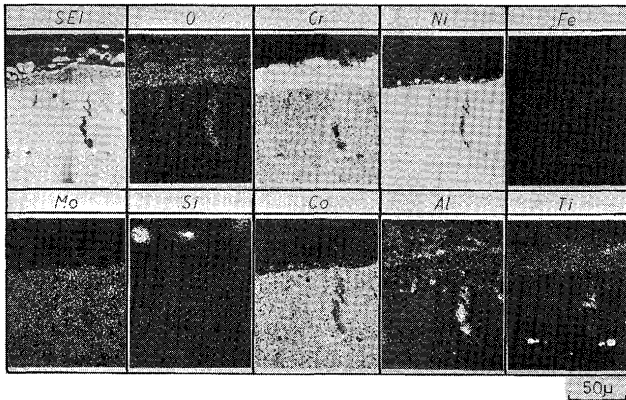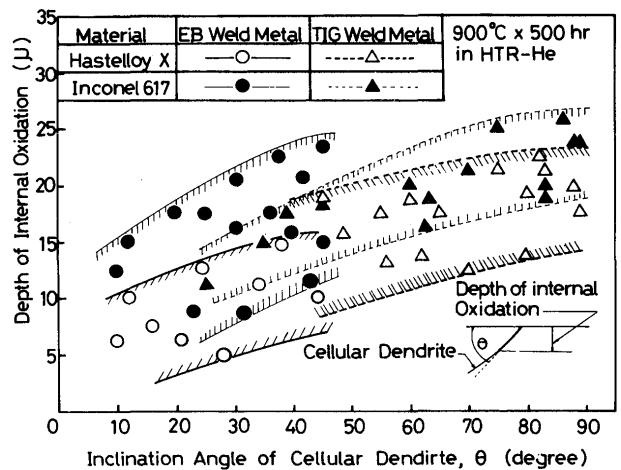
hours. The composition of O, Al and Ti is rich at the grain boundaries, showing that the internal oxidation is mainly composed of Al and Ti oxides.

The Maximum internal oxidation depth of base metal

and its electron beam and TIG weld metal is shown in **Fig. 5** to **Fig. 7** respectively. They show the same tendency as in the case of weight gain and the maximum depth of internal oxidation increases parabolically against the aging time. Furthermore, the resistance of each material against the internal oxidation corresponds to the case of weight gain, and Hastelloy X shows the most excellent internal oxidation resistance amoung the materials used.

When the maximum internal oxidation depth of electron beam and TIG weld metal is compared to that of base metal for the respective materials, there is little difference from the base metal in the case of electron beam weld metal but the maximum internal oxidation depth of TIG weld metal is generally larger than the base metal and electron beam weld metal. Especially, their differences are clearly noted in the case of aging at 900°C for 3,000 hours. The internal oxidation produced in the weld metal usually progresses along the cellular dendrite and it appears that the larger the inclination angle θ which is made between a cellular dendrite and the surface of test specimen, the deeper the internal oxidation progresses generally. This relation is shown in **Fig. 8** for the weld

Fig. 5 Relation between aging time and max. depth of internal oxidation for base metal
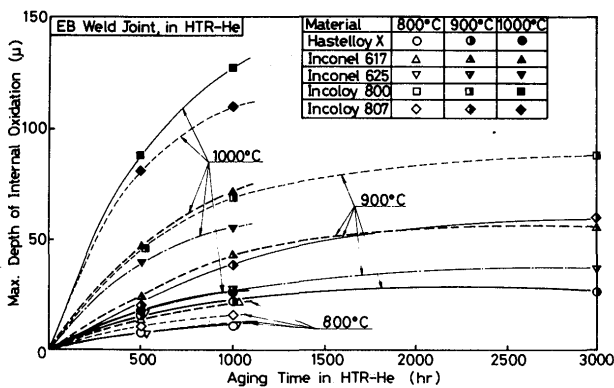
Fig. 6 Relation between aging time and max. depth of internal oxidation for electron beam weld metal

Fig. 8 Relation between angle of cellular dendrite and depth of internal oxidation

metal of Hastelloy X and Inconel 617 aged at 900°C for 500 hours. This reveals that θ of TIG weld metal is generally larger than that of electron beam weld metal and so, the internal oxidation depth of TIG weld metal is larger than that of electron beam weld metal.
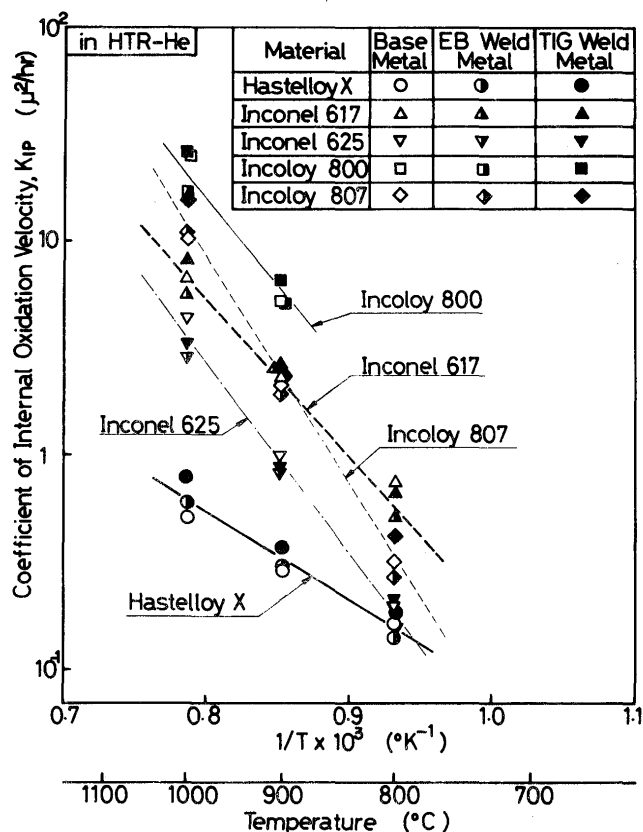
Figure 9 shows the coefficient of internal oxidation

Fig. 9 Relation between temperature and coefficient of internal oxidation velocity

velocity against the test temperature for each material. Assuming that the maximum internal oxidation depth follows the parabolic rule against the time, the coefficient of internal oxidation velocity K_{IP} was calculated from the following relation.

$$\Delta D^2 = K_{IP}.t + C,$$

where

ΔD: Maximum internal oxidation depth (μ)
at aging time t,

t; Aging time (Hr),

K_{IP}, C: Constant

The temperature dependence of K_{IP} on each material shows nearly linear relation in the Arrhenius' indication. K_{IP} values of TIG weld metal for each material are

generally larger than those of base metal and electron beam weld metal, and K_{IP} values of electron beam weld metal are equivalent to or below those of base metal. This tendency is considered to be resulted from the directivity of cellular dendrite of weld metal which was stated above.

In the case of Hastelloy X, a slope of K_{IP} against temperature is very gentle as compared to those of other materials, showing that a progressive rate of internal oxidation with a rise of temperature is smaller than those of other materials.

4.3 Adherence peoperty of oxide film

The adherence property of surface oxide film is also an important factor to evaluate the corrosion resistance of material in high temperature helium. Because if the oxide film peels off, the environment will contact to the matrix, of material directly to promote a local corrosion such as internal oxidation and if the oxide film peels off and is mixed in helium, it pollutes the internal core of nuclear plant and especially, when a radioactive substance such as Co exists in the oxide film, it causes a serious problem in safety.

Hastelloy X shows the most excellent abherence proerty among the materials used for the test. As an example, Photo 1 shows the scanning electron micro-

Base Metal—|—Weld Metal   Base Metal—|—Weld Metal
        200μ   500μ
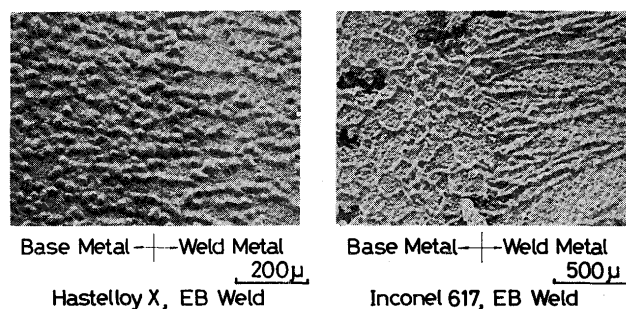Hastelloy X, EB Weld   Inconel 617, EB Weld

Photo. 1 SEM image of the surface of electron beam weld zone aged at 900°C in helium for 3000 hr

photographs of specimen's surface of electron beam weld zone of Hastelloy X and Inconel 617 aged at 900°C in helium for 3,000 hours. The surface oxide film of Hastelloy X is strongly adhered and no peel-off of oxide film is discovered at all while there is a trace of peel-off on the surface oxide film in the case of Inconel 617, irrespective of base metal or weld metal.

4.4 Distribution of compositions

The line analysis by EPMA was carried out on the cross-section of each material after aging in helium, from

the matrix to the surface oxide film. An example of the results is shown in **Fig. 10**. Al, Ti, Cr and O are rich in the oxide film, showing that the oxide film is composed of Al, Ti and Cr oxides. Fe, Ni, Co, Mo and Si are scarcely contained in the oxide film. Among these compositions, Si may become rich in another position of oxide film and is unstable as a composition in the oxide film. The compositions contained in the oxide film can be easily presumed from the oxidation potential figure shown in Fig. 2.

Regarding the composition change from the matrix to the boundary of matrix oxide film, Cr shows the characteristic aspect, that is, at the boundary the relative intensity of Cr decreases by approximately 7 to 10% as

those under the aging condition at 900°C for 3,000 hours. In addition, in this aging condition the cellular dendrite in the weld metal nearly disappears. Under the compared to that of the matrix and negative concentration slope of approximately 50μ is formed in a specimen's thickness direction. Corresponding to this, Fe and Ni form the positive concentration slope from the matrix to the boundary. When the electron beam and TIG weld metals are composed to the base metal for each material, there was no notable difference in the distribution and dispersion of each compositon.

A change of composition distribution in the oxide film by aging is well represented in a change of relative intensity of Cr and Al. As an example, Cr distribution for
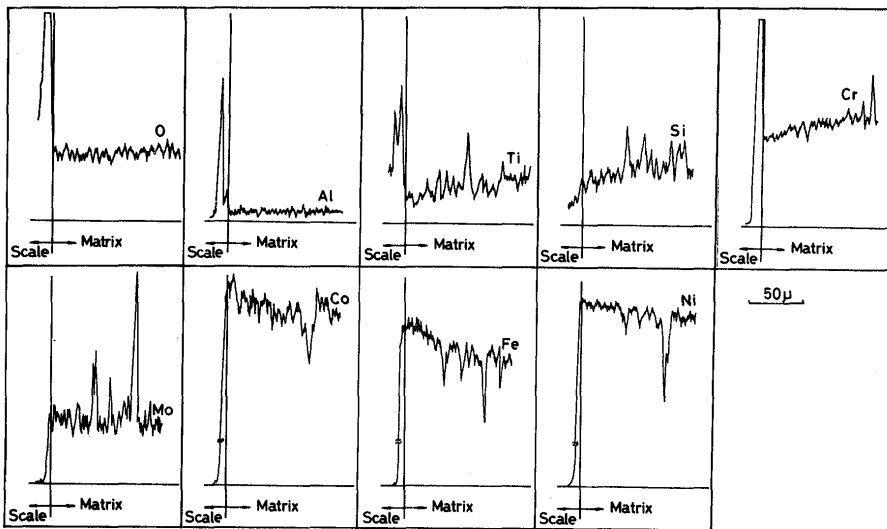
Fig. 10 Distribution of compositions for electron beam weld metal of Hastelloy X aged at 900°C in helium for 500 hr

Fig. 11 Distribution of Cr for electron beam weld metal of aged Hastelloy X

or the longer the aging time, the larger the relative intensity of Cr in the oxide film becomes and the wider the thickness of oxide film becomes. This is considered to correspond to increase in weight gain of oxide film.

4.5 Structure and hardness

As an example, **Table 8** shows the cross-sectional microstructure of Hastelloy X under various aging conditions. Under the aging condition at 800°C for 500 hours, a large number of fine-grained carbides are already precipitated at the grain boundaries and in the matrix. In the case of weld metal, many carbides are precipitated in the cell boundaries of cellular dendrite. At 900°C, there occurs the cohesion of precipitated carbides, and the longer the time elapses, the more the cohesion progresses. Under the aging condition at 1,000°C for 500 hours, the cohesion of carbides is more remarkable as compared to
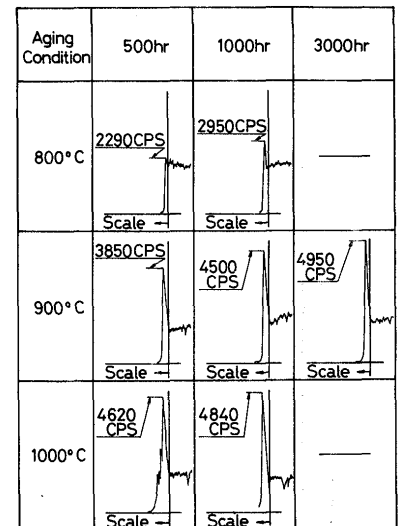
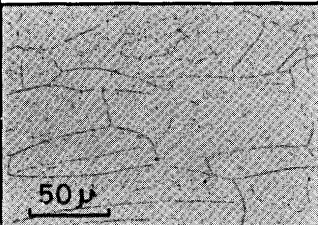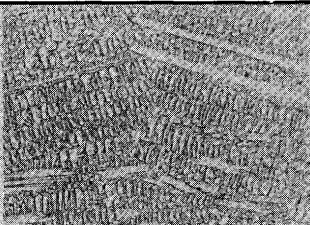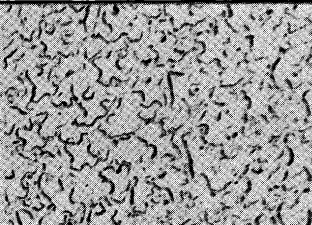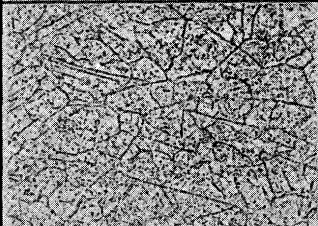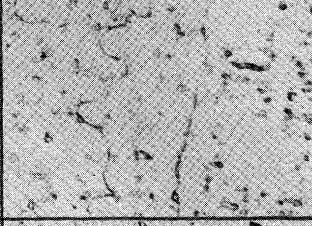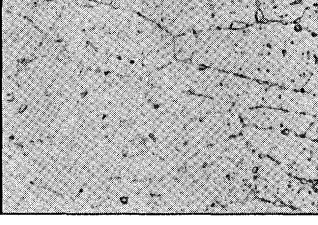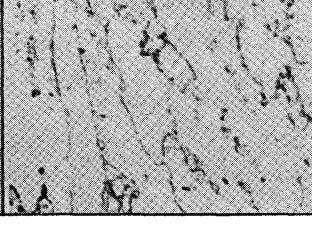electron beam weld metal of aged Hastelloy X is shown in **Fig. 11** It reveals that the higher the aging temperature aging condition at 1,000°C for 1,000 hours, the precipitated carbides in the matrix decrease considerably and the cohesion of rough carbides in the matrix decrease considerably and the cohesion of rough carbides is remarkable at grain boundary. It is reported that these precipitated carbides in Hastelloy X are found to be M_6C by X-ray diffraction analysis[2,3].

For other superalloys, a tendency of precipitation process of carbides by aging was similar to the case of Hastelloy X.

Figure 12 shows the hardness change of Hastelloy X by aging. Each plot show an average of micro vickers hardness (load: 200g) measured at 7 to 10 points at the center of the matrix. The hardness changes of base metal and its electron beam and TIG weld metal show a similar tendency regardless of some dispersions. Under the aging

Table 8 Cross-sectional microstructure for base and weld metals of aged Hastelloy X

Aging Condition		Base Metal	EB Weld Metal	TIG Weld Metal
Not Aged		50 μ		
800°C	500 hr			
900°C	500 hr			
	1000 hr			
1000°C	500 hr			
	1000 hr			

condition at 800°C for 500 hours or at 900°C for 500 hours, the hardness of matrix increases with precipitation of carbides as compared to that of not aged matric, and when the aging time becomes further longer, it tends to be softened, and under the aging condition at 900°C for 3,000 hours, the hardness of matrix becomes close to that of not aged one. This is presumed to correspond to cohesion and roughing of carbides by over-aging. At 1,000°C, the over-aging is further remarkable, and at the aging time of 500 hours, the hardness is already softened than that of the not aged material. The same tendency was noted for other materials.

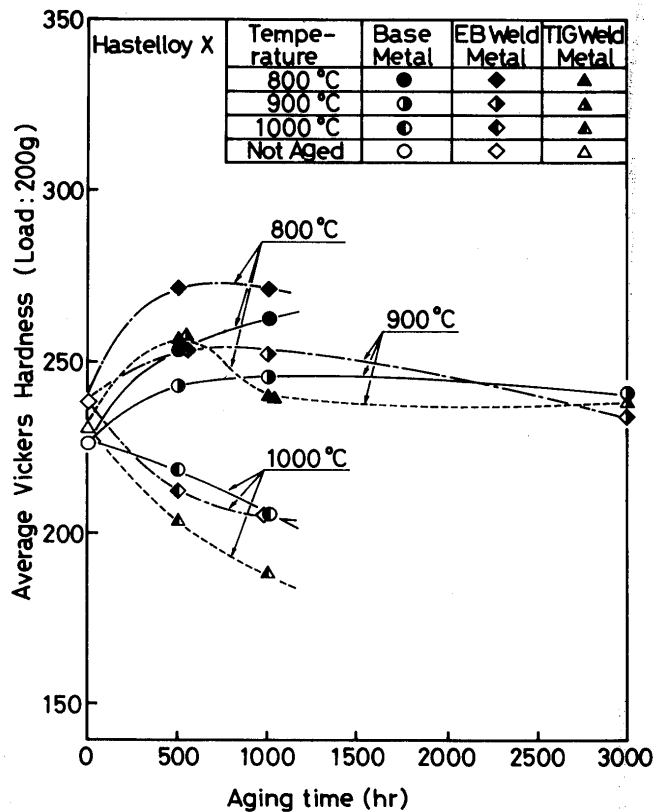| Hastelloy X	Tempe-rature	Base Metal	EB Weld Metal	TIG Weld Metal
	800 °C	●	◆	▲
	900 °C	◑	◈	▲
	1000 °C	◐	◆	▲
	Not Aged	○	◇	△

Fig. 12 Relation between aging time and average vickers hardness for Hastelloy X

5. Conclusion

In this paper, the environmental effect of weld zone of heat-resistant superalloys by aging in high temperature helium was examined. The results are summarized as follows.

(1) Hastelloy X showed the most smallest weight gain among the materials used, and no difference was discovered among the base metal, the electron beam weld joints and TIG weld joints for the respective materials.

(2) Regarding the internal oxidation resistance, the electron beam weld metal was equivalent to or superior to the base metal, while the TIG weld metal was generally inferior to it. Among the materials used, Hastelloy X showed the most excellent internal oxidation resistance.

(3) The oxide film of Hastelloy X showed the most excellent adherence property among the materials used.

(4) Concerning the process of carbides precipitation, it follows the precipitation and cohesion with a rise of aging temperature and a lapse of aging time, and a change of hardness corresponds to it. However, notable difference of the precipitation processes was not noted among the base metal and electron beam weld metal and TIG weld metal.

References

1) Report of the 122nd and 123rd Committee of JSPS(1974), p.21

2) Report of the 122nd and 123rd Committee of JSPS(1972), p.69

3) Susukida, Tsuji and Kawai, "Properties of Solution Strengthened Nickel Base Alloys in the Process of Long-time and High-temperature Heating", Report of the 123rd Committee of JSPS, Vol.17, No.3(1976), p.319-329.